Heat and Mass Transfer (2019) 55:353–374
https://doi.org/10.1007/s00231-018-2425-0

ORIGINAL

Multi-objective optimization of the basic and single-stage Organic Rankine Cycles utilizing a low-grade heat source

Mert Sinan Turgut[1] · Oguz Emrah Turgut[1]

Received: 15 February 2018 / Accepted: 9 July 2018 / Published online: 13 July 2018

Abstract

This study deals with the multi-objective optimization of basic and single-stage Organic Rankine Cycles (ORC) utilizing a low-grade heat source. Twelve different isentropic and dry pure refrigerants are considered as the primary working fluid for two different ORC configurations. Specific Investment Cost (SIC) and second law efficiency of the thermodynamic cycle are considered for optimization objectives to be optimized seperately and concurrently. Sixteen and twenty two different decision variables are respectively taken into account for modeling of the basic and the single-stage ORC optimization problems. The optimization problem is solved by applying a swarm based metaheuristic optimizer called Artificial Cooperative Search (ACS) algorithm. A pareto curve comprised of non dominated optimal solutions is constructed for each refrigerant-cycle pair and the best answer among the set of non dominated solutions are chosen by means of TOPSIS decision making method. Thermodynamic performance of each refrigerant are evaluated with respect to numerical outcomes of the objective functions. Comparative analysis based on the efficiencies of problem objectives reveals that R236ea, R245fa and R600 are selected as the best performers of the basic ORC and R245ca, R245fa and R600 are selected as the best performers of the single-stage ORC. Finally, a sensitivity analysis is executed to observe the effect of the decision variables on the objectives. It is understood that the evaporator shell diameter, number of tube passes in the evaporator, evaporator pressure and mass flow rate of the refrigerant are the decision variables with the most influence on the design objectives.

Keywords Artificial cooperative search · Multi-objective optimization · Organic Rankine Cycles · Refrigerants · Thermal design

List of symbols

A	Heat exchanger surface (m^2)
ACS	Artificial cooperative search
B,C,K	Constants of the economical model
Bo	Boiling number
C	Cost ($)
C_p	Spesific heat at constant pressure (J/kgK)
d	Diameter (m)
f	Friction factor
F	Factor of the economical model
$f()$	Objective function
g	Gravitational acceleration (m/s^2)
GWP	Global warming potential
g()	Inequality constraint
h	Convective heat transfer coefficient (W/m^2K)
h	Enthalpy (kJ/kg)
h()	Equality constraint
I	Irreversibility (kJ)
k	Thermal conductivity (W/mK)
LMTD	Log mean temperature difference (K)
$\dot{m}$	Mass flow rate (kg/s)
M	Molecular mass (kg/kmol)
N,n	Number of component
Nu	Nusselt number
ODP	Ozone depletion potential
ORC	Organic rankine cycle
P	Pressure (Pa)
P_t	Distance between two tubes in the heat exchanger (m)
Pr	Prandtl number
Q	Heat transfer rate (kW)
R	Fouling resistance (m^2K/W)
Re	Reynolds number
s	Entropy (kJ/kgK)

✉ Mert Sinan Turgut
sinanturgut@me.com

[1] Mechanical Engineering Department, Ege University, 35040 Bornova/Izmir, Turkey

SIC	Specific investment cost ($/kW)
SSORC	Single-stage organic rankine cycle
T	Temperature (K).
TC	Total cost ($)
U	Overall heat transfer coefficient (W/m^{2}K)
v	Velocity (m/s)
W	Work (kJ)
x	Vapor quality
X_{tt}	Lockhart-Martinelli parameter
$\vec{x}$	Design variable

Greek letters

η	Efficiency
μ	Viscosity (kg/ms)
ρ	Density (kg/m^3)

Subscripts

0	Ambient
CO,c	Condenser
EV,e	Evaporator
FH	Feed heater
fg	Liquid-vapor phase
g,v	Vapor phase
H	Hot medium
HX	Heat exchanger
in	Inside
l,f	Liquid phase
L	Cold medium
m	Mean
M	Material
Out,o	Outside
PP,p	Pump
r	Refrigerant
tot	Total
TR,t	Turbine
w	Wall

1 Introduction

Organic Rankine Cycle (ORC) is a thermodynamic cycle that can produce mechanical work or electricity from different types of heat sources with employing an organic refrigerant as a working fluid [1]. ORCs possess several advantages over Steam Rankine Cycles (SRC) when a low-grade heat source is utilized. Some of the prominent advantages of ORCs are that they can operate in much lower vaporization pressures and work with more feasible mass flow rates of working fluids [2]. These favourable merits make ORCs less complex, easier to be downsized and more practical and economical compared to SRCs. Furthermore, these advantages pave the way for utilizing more environmentally-friendly heat sources in ORCs, such as solar energy, geothermal energy and waste heat energy.

Proper selection of a working fluid plays a vital role in thermal performance and efficiency of ORCs, particularly for low-grade heat source applications [3, 4]. Working fluids are mainly analyzed and classified in three distinct categories based on their slope of the saturated vapor curve in the temperature-entropy diagram. These three types of working fluids are called wet, isentropic and dry fluids. Wet fluids have a negative slope of the saturation vapor curve and they need to be superheated before entering to the turbine, otherwise, they may enter the turbine in the two-phase state and liquid droplets in the two-phase mixture may corrode the turbine blades. However, isentropic and dry fluids having vertical and positive slope respectively do not need to be superheated before entering to the turbine. Therefore, it can be concluded that isentropic and dry fluids are more preferable than wet fluids as superheating the fluid before entering the turbine will lower the overall cycle efficiency. For more information and detailed analysis over selection of working fluids in low-grade heat source ORCs, distinguished research studies of Abolwefa et al. [4], Desai and Bandyopadhyay [5] and Bao and Zhao [6] can be referred. Abolwefa et al. [4] made a review study on industrial applications of solar Rankine cycles. A considerable part of this mentioned study deals with discussion and literature review on selection of working fluids for low-grade heat source ORCs. Desai and Badyopadhyay [5] reported a comparative analysis of the effect of different working fluids on thermo-economical performance of solar Rankine cycles. Mentioned study includes a broad literature review on the selection of working fluids for low-grade heat source and solar Rankine cycles. Bao and Zhao [6] made a review study over selection of working fluids and expanders for low- and medium-grade heat source ORCs. In their review paper, they made a broad discussion on the impact of various working fluids on the performance of different types of ORCs.

Design optimization of ORCs has been becoming a significant research area and widely discussed by plenty of researchers in the literature. Xi et al. [7] studied the thermal design optimization of three different types of ORCs, namely basic ORC (BORC), single-stage regenerative ORC (SRORC) and double-stage regenerative ORC (DRORC) with considering exergy efficiency as an objective function to be optimized by Genetic Algorithm. Turbine inlet pressure and temperature and fraction of flow rates at each regenerative stage are considered as decision variables those to be iteratively varied during heuristic search proces. Six different working fluids are employed for each system configuration and numerical results showed that R11 and R141b gave the best performance in terms of thermal efficiency. Hayat et al. [8] carried out a dual-objective optimization study of basic and recuperative organic Rankine cycles. The authors employed seven organic fluids for the basic ORC and four dry fluids for the recuperative ORC. Two objectives, namely the cost and the first law efficiency of the cycle, and four decision variables are

considered for the optimization problem. The authors have applied the NSGA-II algorithm to solve the dual-objective optimization problem and found out that for the basic ORC, R21 outperformed other refrigerants in case of thermal efficiency while R245ca surpassed other refrigerants in terms of cost and for the recuperative ORC, R601 is a viable refrigerant to employ in the cycle in terms of thermal efficiency while R236ea is viable cost wise. Yilmaz et al. [9] performed a thermal efficiency analysis of an ORC with an internal heat exchanger by utilizing a Artificial Neural Network (ANN). The authors have analyzed thermal performances of two refrigerants, R410 and R407c. The ANN is trained with four inputs, evaporator, condenser, subcool and superheat temperatures, and one output, first law efficiency of the cycle. The ANN is trained for various configurations and the one with the lowest R^2-value has been selected for the comparison with the experimental results. The authors have reported the desirable input variable values for higher thermal efficiency and preferable ANN configuration in the paper.

Pierobon et al. [10] conducted a multi-objective optimization of MW-size ORC for waste heat recovery. They used Genetic Algorithm for the optimization process as thermal efficiency, total volume of the system and net present value are considered for three objectives functions for the multi-objective optimization problem. Various type of refrigerants were used for cycle configurations and it was observed that cyclopentane and acetone are the best performing working fluids. Kazemi and Samedi [11] examined a new ORC that is inspired from three different ORC configurations. They considered thermodynamic efficiencies and spesific investment cost as optimization objectives. Considered design parameters were evaporator and regenerative temperatures, pinch point temperature difference of evaporators and degree of superheat. Working fluids of Isobutane and R123 were seperately applied to the ORC system and their thermodynamic performances were also compared in terms of first and second law efficiencies. Exhaustive comparison between different design conditions and configurations revealed that there occurs a marked increase in thermal and exergy efficiencies and significant decrease in exergy destruction rates, particularly in the evaporator section for both fluids compared to preliminary ORC types.

Andreasen et al. [1] approached the optimization of ORCs from a different point of view and introduced the working fluid as an optimization parameter. Two case studies were performed, one with 120 °C and the other with 90 °C hot fluid inlet temperature. Effects of various pure and mixture fluids on ORC system design parameters were investigated. By examining the results, it was concluded that mixtures can increase the net work output and reduce the pressure levels. Numerical investigations also showed that using mixtures rather than pure fluids entails a significant amount of increase in net power output and a reduction in the working pressure levels. In addition, it was observed that process fluids having critical temperatures close to half of the hot fluid inlet temperature give the maximum net power output. Yang and Yeh [12] investigated the economic optimization of an ORC working with a geothermal heat source. An economic performance parameter called net power output index was introduced and optimization of the ORC was performed with zero ODP and lower GWP working fluids. The results showed that R600 gives the most optimistic outcomes regarding to thermal and environmental aspects. It was also seen that employing R600a or R1233zd as working fluid result in a considerable decrease in equipment cost rates. Khaljani et al. [13] performed a multi-objective optimization for a regenerative system to determine the optimum design parameters. Exergy efficiency and total cost rate are selected as design objectives to be solved by Non-dominated Sorting Genetic Algorithm-II (NSGA-II) optimization algorithm. The proposed cycle consists of a gas turbine and a basic ORC. It was reported in the paper that exergetic efficiency is increased from 51.4 to 56.5 and 12.98% reduction in total cost is achieved with multi-objective optimization case compared to the preliminary case. Imran et al. [14] studied the multi-objective optimization of basic, single-stage regenerative and double-stage regenerative ORCs under constant heat source condition. NSGA-II is utilized as the optimization algorithm and thermal efficiency and spesific investment cost are selected as the problem objectives. Optimization case studies are performed for each three cycle considering five different working fluids of R123, R11, R245fa, R141b and R134a. The results showed that R245fa is the best performing working fluid.

In this paper, multi-objective optimization of a basic and a single-stage ORC making use of a low-grade heat source is extensively studied. A group of twelve different refrigerants consisting of dry and isentropic fluids are benefited as working fluids for both cycle configuration. The first objective considered for the optimization problem is the Spesific Investment Cost (SIC), which is an index that indicates the cost of generating 1 kW of electrical energy. The second objective considered is the second law efficiency of the cycle. Sixteen and twenty two design variables are taken into consideration, respectively, for the optimization of the basic and single-stage ORCs. Pareto frontier of each working fluid-cycle pair is generated by applying the Artificial Cooperative Search (ACS) [15] algorithm to the multi-objective optimization problem. ACS algorithm is a metaheuristic optimization algorithm based on the interaction between two populations which are in prey-predator kind of relationship. The ACS algorithm has favorable exploration capabilities and also is able to converge to optimum points even in a large search domain. Best answer in the Pareto frontier comprised of non-dominated solutions is chosen by means of the TOPSIS multi-criteria decision making method and sensitivity analyses of the best performing three working fluids for each cycle are discussed. Thermoeconomic performances of twelve different working fluids are examined for both cycle configuration and their corresponding Pareto

frontiers resulted from multi objective optimization are explicitly evaluated, which have not been implemented and discussed yet in the literature with a such detailed examination. This research mainly aims to obtain the optimal design configuration of the basic and single-stage ORCs considering the concurrent effects of design objectives of second law efficiency and SIC of the thermodynamic system.

To the best of the authors' knowledge, there is no avaliable research study in the literature that considering in-depth design aspects of the basic and single-stage ORCs, such as design configuration of the heat exchangers, at the same time taking into account of influences of different working fluids over thermal system efficiencies. This kind of evaluation will allow to maintain much more efficient power generation systems with taking into account of running cost issues. Rest of the paper is organized as follows: fundamental procedure for modeling of the ORCs is given in the second section, multi-objective optimization problem and the basics of the ACS algorithm are briefly presented in the third section, optimization results and sensitivity analyses are reported and discussed in the fourth section and the paper is concluded with remarkable comments with the fifth section.

2 Modeling and description of the organic Rankine cycle

2.1 Brief description of the organic Rankine cycle

Fig. 1 show the schematic and the temperature-entropy diagrams of a basic and a single-stage ORC, using a low grade heat source to accomplish the evaporation process in the evaporator. A basic ORC consists of four distinct processes as seen in Fig. 1. These are heat addition to the refrigerant in the evaporator (process 1–2), pressure drop and expansion of the refrigerant resulting in power generation in the turbine (process 2–3), heat removal from the refrigerant (process 3–4) and pumping process which allows the circulation of the refrigerant in the cycle (process 4–1). Lines on the top and the bottom of the saturation curve (lines 6–5 and 8–7) respectively represent the temperature drop of the transport fluid that transfers the heat from the low-grade heat source to the refrigerant in the evaporator and temperature increase of the cooling fluid in the condenser. In the single-stage ORC, some amount of refrigerant is withdrawn during a specific stage of the expansion process and directed to the feed heater. This refrigerant is then consequently used for regenerative purposes to supply heat the remainder of the refrigerant that completes the expansion process, releases the excess heat at the condenser and then compressed at the first pump. Following that, after the heat transfer at the feed heater occurs, the second pump compresses and circulates the refrigerant at the high pressure cycle.

In this study, twelve pure refrigerants are selected as working fluids to be compared against each other with regard to thermoeconomic and thermodynamic aspects. All considered working fluids are either dry or isentropic refrigerants since wet refrigerants require extra superheating, which resulting in a deterioration in the cycle performance. Thermal properties of the refrigerants used in this study are given in Table 1. Some design constraints are also imposed on thermal design problem in order to ensure the feasibility and efficiency of the optimized ORC system. One design issue that should be given an utmost concern is to take the upper evaporator pressure limit as 90% of the critical pressure of the working fluid. Imposed constraints on design parameters and their influences on problem objectives will be explicitly discussed and evaluated in the upcoming sections.

In order to simplify the modeling and analysis of the cycles and decrease the computational load burden caused by the excessive redundant calculations, the following assumptions have been made [16].

1. Each considered cycle operates under steady-state conditions and the thermodynamic state of the refrigerant at the outlet of the condenser and evaporator is assumed to be saturated.
2. All pressure and heat losses throughout the refrigeration system are neglected and disregarded.
3. Heat exchangers and feed heater are selected as shell and tube type.
4. Influences of the kinetic and potential energies on the thermodynamic analysis are disregarded.
5. Fully developed flow is considered to calculate the heat transfer parameters.

2.2 Thermodynamic and economical modeling of the organic Rankine cycle

Based on the above given assumptions and simplifications, thermodynamic modeling of each component in the cycle are formalized by following energy, mass balance and irreversibility generation equations. The governing mass balance equations are

$$\sum \dot{m} = 0, \quad \sum x \cdot \dot{m} = 0 \tag{1}$$

the energy balance equation is

$$\sum \dot{Q} + \sum \dot{W} + \sum \left(\dot{m} \cdot h\right) = 0 \tag{2}$$

and the irreversibility equation is

$$I_{1-2} = T_0 \left(S_2 - S_1 - \frac{Q_0}{T_0} - \frac{Q_H}{T_H} \right) = T_0 \Delta S_{net} \geq 0 \tag{3}$$

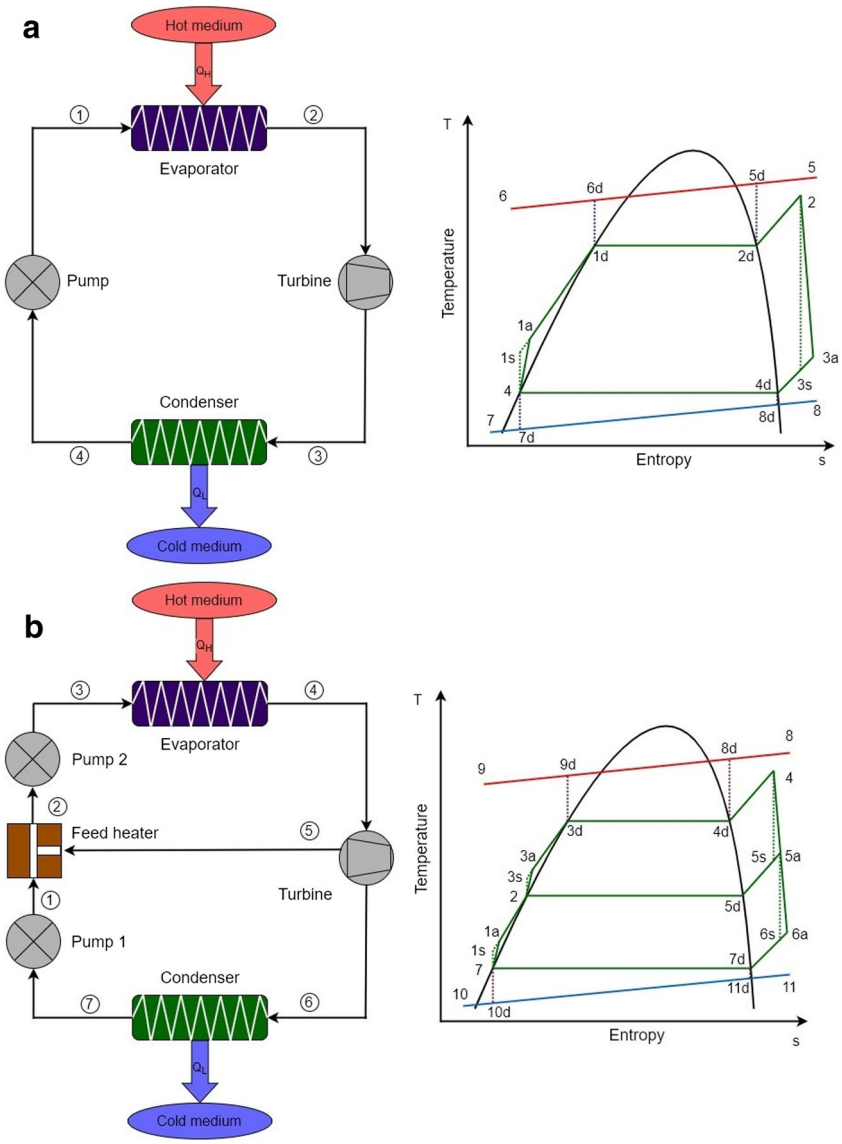

Fig. 1 Schematic representations of the a) basic ORC b) single-stage ORC

Thermodynamic models and irreversibility generation equations of the components of the basic ORC and the two-stage ORC are respectively given in Tables 2 and 3. Numerical values of the isentropic turbine efficiency (η_t), the isentropic pump efficiency (η_p) and the ambient temperature (T_0) are correspondingly taken as 0.80, 0.75 and 298.15 *K*. Moreover, mechanical pump efficiency and mechanical turbine efficiency are correspondingly taken as 0.95 and 0.97 while mass flow rate of the coolant in the condenser is 4.0 *kg/s*. Interested readers can consult [18] for the economical modelling of the cycle.

2.3 Heat exchanger modeling and design

It can be comprehended from the economical model equations that design of the heat exchanger plays a critical role in determining the investment cost of the cycle. Therefore, thermal design and modeling of the heat exchanger should be carefully studied and utmost concern should be given to proper usage of the correct heat transfer correlation. For both cycle design configuration, two phase heat transfer occurs in the evaporator, the condenser and the feed heater. In this study, the condenser, the evaporator and the feed heater are modeled as shell and tube heat exchangers. Cooling water is employed as the secondary working fluid at the condenser while Therminol VP-1 is used to transfer the heat from the low-grade heat source to the primary fluid of the cycle at the evaporator. Mass flow rate of the Therminol VP-1 is taken as 1.0 *kg/s* in numerical simulations. The coefficients for the calculating the number of tube passes of the shell and tube heat exhangers can be obtained from [19].Table 4 reports the correlations used for the calculation of the convective heat transfer coefficient of each flow in the cycle. Heat exchange area of each heat exchanger for the given heat load is calculated by the following expression

Table 1 Thermal properties of the working fluids used in this study [16, 17]

Refrigerant	Critical Temperature (K)	Critical Pressure (kPa)	ODP	GWP	Type of fluid
R123	456.81	3672.0	0.06	77	isentropic
R134a	374.21	4059.2	0.00	1430	isentropic
R141b	477.50	4212.0	0.12	725	isentropic
R227ea	374.90	2925.2	0.00	3220	Isentropic
R236ea	412.44	3420.0	0	710	dry
R236fa	398.07	3200.0	0	9810	isentropic
R245ca	447.57	3940.7	0	693	dry
R245fa	427.01	3651.0	0	710	isentropic
R600	425.12	3796.0	0	20	dry
R600a	407.81	3629.0	0	20	dry
R601	469.70	3370.0	0	20	dry
R1234yf	367.85	3382.2	0	4	isentropic

$$A = \frac{\dot{Q}}{U \Delta T_{LMTD}} \tag{4}$$

where A is the required heat exchanger surface, ΔT_{LMTD} is the logarithmic mean temperature difference for the corresponding heat exchanger and U is the overall heat transfer coefficient and can be calculated by the following expression

$$U = \frac{1}{\left[\left(\frac{d_{out}}{d_{in}}\right)\left(\frac{1}{h_{in}}\right) + \left(\frac{d_{out}}{d_{in}}\right)R_{in} + \left(\frac{d_{out}}{2k}\right)\ln\left(\frac{d_{out}}{d_{in}}\right) + R_{out} + \left(\frac{1}{h_{out}}\right)\right]} \tag{5}$$

2.4 Validation and verification of the ORC model

Numerical outcomes of the proposed model is compared with two other basic and two-stage ORCs studies in the literature in order to validate the accuracy of the thermodynamic model used in this study. These two literature thermodynamical modeling approaches were made by Imran et al. [14] and Safarian and Aramoun [24]. Safarian and Aramoun [24] presented energy and exergy assessment of the basic and modified ORCs. The researchers used R113 as the working fluid and performed an exergetic evaluation of the basic and modified ORCs and investigated the effect of the evaporator pressure on the system under given operating conditions. The effect of the evaporator presssure on the cycle efficiencies were compared for the proposed model in this study and the model in Safarian and Aramoun [24] in Fig. 2 for the same operating conditions. It can be seen from the Fig. 2 that for both cycles, the largest error is not more than 1.5%. In the other work, Imran et al. [14] performed a multi-objective optimization study for the basic, single-stage regenerative and double-stage regenerative ORCs. They used five different working fluids for each considered design configuration and performed a sensitivity analysis with various design parameters by utilizing R245fa as a working fluid. Variation of the ORC cycle efficiency with the evaporator pressure for the proposed model in this study and for the model presented in Imran et al. [14] are compared for the same operating conditions in Fig. 3. It can be seen from the Fig. 3 that the largest error is around 1.3% for both cycle design.

3 Multi-objective optimization

Many real-world optimization problems are non-linear with having more than one conflicting objectives [25]. Engineers and scientists have long been trying to solve these kind of

Table 2 Thermodynamic model and irreversibility generation of each components in the basic ORC

Evaporator	$\dot{Q}_e = \dot{m}_r.(h_2 - h_1)$ $\dot{I}_e = T_0.\dot{m}_r.(s_2 - s_1 - (h_2 - h_{1a})\ /T_H)$ where $T_H = \frac{T_{5d} + T_{6d}}{2}$
Turbine	$\dot{W}_t = \dot{m}_r.\eta_t.(h_2 - h_3)$ $\dot{I}_t = T_0.\dot{m}_r.(s_{3a} - s_2)$
Condenser	$\dot{Q}_c = \dot{m}_r.(h_4 - h_3)$ $\dot{I}_c = T_0.\dot{m}_r.(s_4 - s_{3a} - (h_4 - h_{3a})\ /T_L)$ where $T_L = \frac{T_7 + T_8}{2}$
Pump	$\dot{W}_p = \frac{\dot{m}_r.(h_1 - h_4)}{\eta_p}$ $\dot{I}_p = T_0.\dot{m}_r.(s_{1a} - s_4)$

Table 3 Thermodynamic model and irreversibility generation of each component in the two-stage ORC

Refrigerant fraction at the outlet of the first stage turbine	$x_t = \frac{h_2 - h_{1a}}{h_{5a} - h_{1a}}$
Evaporator	$\dot{Q}_e = \dot{m}_r.(h_4 - h_3)$
	$\dot{I}_e = T_0.\dot{m}_r.(s_4 - s_{3a} - (h_4 - h_{3a}) \ / T_H)$ where $T_H = \frac{T_{8d} + T_{9d}}{2}$
Turbine 1	$\dot{W}_{tI} = \dot{m}_r.\eta_t.(h_4 - h_5)$
	$\dot{I}_{t1} = T_0.\dot{m}_r.(s_{5a} - s_4)$
Turbine 2	$\dot{W}_{tII} = \dot{m}_r.\eta_t.(1 - x_t)\ .(h_5 - h_6)$
	$\dot{I}_{t2} = T_0.\dot{m}_r.(1 - x_1)\ (s_{6a} - s_{5a})$
Condenser	$\dot{Q}_c = \dot{m}_r.(1 - x_1)\ .(h_6 - h_7)$
	$\dot{I}_c = T_0.\dot{m}_r.(1 - x_1)\ .(s_7 - s_{6a} - (h_7 - h_{6a})\ / T_L)$ where $T_L = \frac{T_{10} + T_{10d}}{2}$
Pump 1	$\dot{W}_{pI} = \frac{\dot{m}_r.(h_1 - h_7).(1 - x_1)}{\eta_p}$
	$\dot{I}_{p1} = T_0.\dot{m}_r.(1 - x_1)\ .(s_{1a} - s_7)$
Pump 2	$\dot{W}_{pII} = \frac{\dot{m}_r.(h_3 - h_2)}{\eta_p}$
	$\dot{I}_{p2} = T_0.\dot{m}_r.(s_{3a} - s_2)$
Feed heater	$\dot{Q}_{fh} = \dot{m}_r.(1 - x_1)\ .(h_2 - h_1) + \dot{m}_r.x_1.(h_5 - h_2)$
	$\dot{I}_{fh} = T_0.((1 - x_1)\ .\dot{m}_r.(s_2 - s_{1a}) + \dot{m}_r.x_1.(s_2 - s_{5a}))$
First and second law efficiencies	$\dot{I}_{tot} = \dot{I}_e + \dot{I}_c + \dot{I}_{p1} + \dot{I}_{p2} + \dot{I}_{t1} + \dot{I}_{t2}$
	$\dot{W}_{net} = \dot{W}_{t1} + \dot{W}_{t2} - \dot{W}_{p1} - \dot{W}_{p2}\ \ \eta_I = \frac{\dot{W}_{net}}{\dot{Q}_e}\ \eta_{II} = \frac{\dot{W}_{net}}{\dot{Q}_e}$

problems having possible alternative solutions which are non-dominated to each other and trade-off between the contradictory design objectives. An improvement made on one of the problem objective worsens the solution quality of the other conflicting objectives. In situations like this, where it is not possible to state a solution is better than the other as in single objective optimization problems, a Pareto curve compiled from non dominated solutions is constructed to observe the spatial distribution of optimal solutions over the design objectives domain. Two different mathematical approaches have been generally developed to solve multi-objective optimization problems. The classical approach turns the multi-objective optimization problem into a single-objective one by scalarizing the each solution by giving them weights that depicts the influence of the objective on the solution while the evolutionary approach treats the problem as it is and directly

Table 4 Convective heat transfer correlations for each type of flow

Correlation	Description	Formulation
Gnielinski [20]	Used for single phase heat transfer taking place evaporator, condenser and feed heater	$v_m = \frac{\dot{m}/\rho}{\left(\frac{N_{tube}}{N_{pass}}\right)\left(0.25\pi d_{in}^2\right)}\ \mathrm{Re} = \frac{\rho v_m d}{\mu}\ \mathrm{Pr} = \frac{C_p \mu}{k}$
Florides et al. [21]	Equations for calculating heat transfer coefficients for hot and cold sides in the evaporator, condenser and feed heater	$h = \frac{f}{8}(\mathrm{Re} - 1000)\left[\frac{f}{8}\right]\ \frac{f}{8} f = (0.79\ln(\mathrm{Re}) - 1.64)^{-2}$ $d_H = d_{out} - d_{in}$ For annulus flow: $\mathrm{Re}_H = \frac{\dot{m} \cdot d_H}{A \cdot \mu}$ $h \leftarrow \{\ 3.66 \cdot k/d_H \leftarrow if\ (\mathrm{Re}_H < 2300)$ Apply Gneilinski equation$\leftarrow$ *else* For intube flow: $\mathrm{Re}_{in} = \frac{4.0\dot{m}}{\pi d_{in} \mu_l}$ $h \leftarrow \{\ 3.66 \cdot k/d_{in} \leftarrow if\ (\mathrm{Re}_{in} < 2300)$ Apply Gneilinski equation$\leftarrow$ else
Gnielinski [22]	Used for calculating convective heat transfer coefficient for out-tube condensation in the condenser and the feed heater	$h = 0.725\left[\frac{\rho_f\left(\rho_f - \rho_v\right) h_{fg} k_f^3 g}{n \mu_f D_0 \left(T_{sv} - \overline{T}_w\right)}\right]^{1/4}$
Gungor and Winterton [23]	Used for calculating convective heat transfer coefficient for in-tube evaporation in the evaporator	$E = 1 + 24000 Bo^{1.16} + 1.37(1/X_{tt})^{0.86} S = \frac{1}{1 + 1.15x10^{-6} E^2 \mathrm{Re}^{1.17}}$ $h_l = 0.023 \mathrm{Re}_l^{0.8} \mathrm{Pr}_l^{0.4} k_l / d$ $h_{pool} = 55 P_r^{0.12} (\log_{10} P_r)^{-0.55} M^{-0.5} q^{0.67}$ $h = E h_l + S h_{pool}$

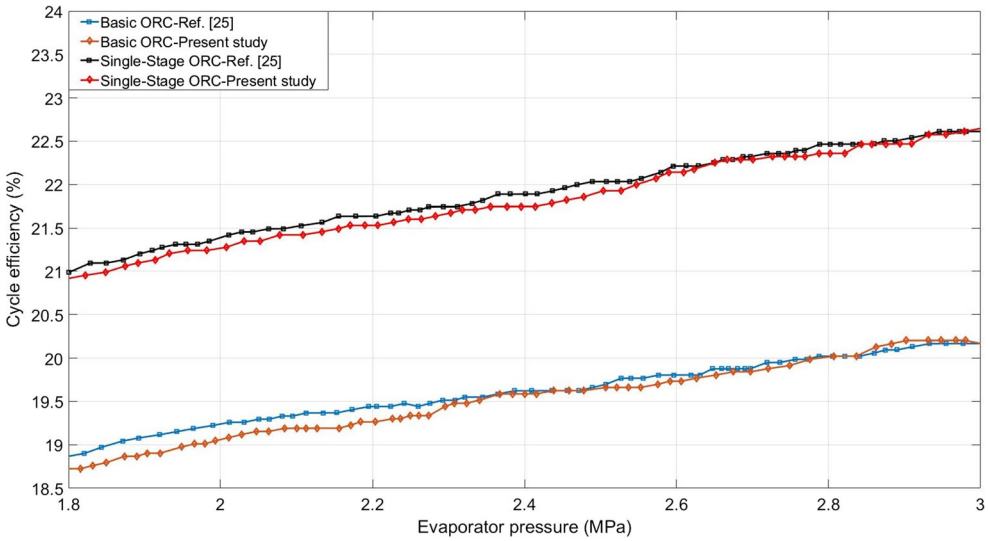

Fig. 2 Validation of the estimation capability of the proposed model with the theoretical data given in Safarian and Aramoun [24]

selects the most appropriate solution from a set of candidate solutions. The classical approach is adopted to solve the multi-objective optimization problem in this study. The pareto curve is scalarized by giving each optimum solution a weight value and TOPSIS multi-criteria decision-making method is utilized to obtain the most desirable solution in the Pareto curve.

Artificial Cooperative Search (ACS) algorithm is utilized to solve the multi-objective basic and single-stage ORC optimization problem by considering the SIC and the second law efficiency as design objectives. ACS is a swarm-intelligence based metaheuristic optimization algorithm. The algorithm deals with the prey-predator relationship of two superorganisms, which are in essence a large group of individuals. In nature, when the amount of food decreases in a habitat, individuals of the same species group up, form a superorganism and migrate to more productive and fertile areas. The migration of the prey superorganism means the inclined level of food for predator individuals as well. Thus, they also form a superorganism and follow the prey superorganism to hunt them. This prey-predator relationship shapes the mathematical concept of the ACS algorithm. Interested readers can consult to the original article for detailed description and mathematical procedure of the algorithm [15]. ACS algorithm is capable of searching large solution spaces and converge to the optimal solution effectively, which reflects the fact that the algorithm has efficient exploration and exploitation capabilities. This superior probing characteristics of the algorithm eases its application in large scale optimization problems with having continuous and discrete decision variables. Therefore, another major aim of this study is to benchmark the optimization performance of ACS over highly-nonlinear real-world multi-objective engineering optimization problem.

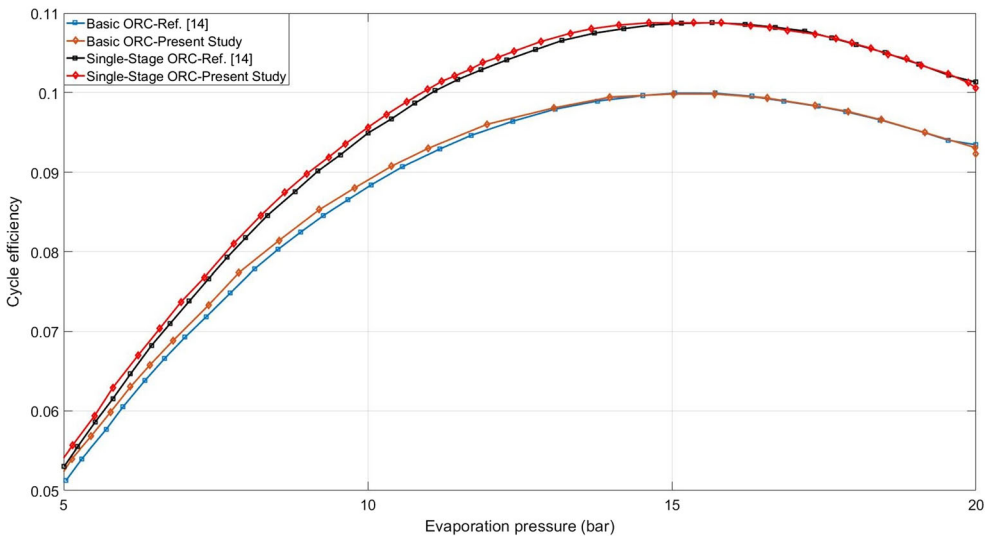

Fig. 3 Validation of the estimation capability of the proposed model with the theoretical data given in Imran et al. [14]

A typical multi-objective optimization problem can be formalized as follows

$$\begin{aligned} &\text{Min/max } f_i\left(\overrightarrow{x}\right) && i = 1,2,\ldots,N \\ &\text{subject to } g_j\left(\overrightarrow{x}\right) \le 0 && j = 1,2,\ldots,M \\ &h_k\left(\overrightarrow{x}\right) = 0 && k = 1,2,\ldots,K \\ &x_m^L \le x_m \le x_m^U && m = 1,2,\ldots,P \end{aligned} \tag{6}$$

where $\overrightarrow{x}$ represents the set of P dimensional decision variables and can be shown as follows

$$\overrightarrow{x} = [x_1, x_2, \ldots, x_P] \tag{7}$$

Furthermore, in Eq. (6), x_m^U and x_m^L represent the upper and lower boundaries of the decision variables respectively and $f_i(\overrightarrow{x})$ represents the N optimization objectives which can be mathematically shown as

$$f\left(\overrightarrow{x}\right) = \left[f_1\left(\overrightarrow{x}\right), f_2\left(\overrightarrow{x}\right), \ldots, f_N\left(\overrightarrow{x}\right)\right] \tag{8}$$

Where $g(\overrightarrow{x})$ and $h(\overrightarrow{x})$ respectively represent the M and K number of inequality and equality design constraints. As previously stated, the classical approach to solve the multi-objective optimization problem is adopted in this study. The "Pareto solutions" are found by varying the weight of the each objective in the solution of the problem, in other words, the Pareto curve is scalarized. TOPSIS method is utilized to select the best answer in the Pareto curve. TOPSIS method is a well-known and well-reputed multi-criteria decision making method that is based on calculating the Eulerian distance between the solution points and the nadir point. Interested readers can consult to Kumar et al. [26] for more information about the TOPSIS method.

Decision variables of the basic and single-stage ORC multi-objective optimization problem and their corresponding upper and lower bounds are respectively given in Tables 5 and 6.

4 Optimization results and sensitivity analysis of the ORC cycle

4.1 Optimization results and discussions

Numerical modeling of thermodynamic cycles and the ACS optimization algorithm are developed in Java environment. Thermodynamic and thermophysical properties of the refrigerants are obtained from the CoolProp library [17]. Because of the stochastic nature of the ACS algorithm, more than one algorithm run is needed to ensure the accuracy of the solution. Therefore, ACS algorithm is executed twenty times for each solution with 30,000 function evaluations for the both cycles. The program is run at a quad-core Intel i5–4460 @ 3.20 GHz with 16.0 GB RAM desktop computer.

Figures 4 and 5 report the Pareto-curves of the basic ORC operated with different refrigerants along with the most desirable solutions selected by the TOPSIS method. Correspoding optimal SIC, second law efficiency and the decision variables of the points with the maximum second law efficiency, minimum SIC and the point selected by the TOPSIS method are respectively given in Tables 7, 8 and 9. Each point in the pareto-curve represents a optimal solution for a specific set of weights assigned to the objectives. It can be seen from the Pareto curves that TOPSIS method chooses the optimal solution that is closer to the minimum SIC rather than maximum second law efficiency value for each cycle configuration. Performance comparison between each cycle running with different refrigerants shows that R245fa, R236ea and R600 give the most satisfactory results. Table 7 reports the minimum SIC, the maximum second law efficiency and the optimum solution found by TOPSIS method for R236ea. As can be seen in Table 7, minimum SIC value of R236ea is 5988.496 *$/kW* and its corresponding second law efficiency is 0.374. Maximum second law efficiency of the mentioned system is 0.465 and its respective SIC value is 31,185.805 *$/kW*. Result retrieved from multi objective optimization by virtue of TOPSIS method is also given at the third column in Table 7. It is observed that TOPSIS result for SIC is 5998.696 *$/kW* while its respective second law efficiency is 0.379. It is also seen that TOPSIS solution is inclined to minimum SIC value. Decision variables such as the condenser and evaporator outer tube diameter and condenser temperature nearly get the same optimal value for both single-objective optimization cases. On the other hand, most of the remaining decision variables except evaporator pressure and superheat temperature hit maximum or minimum allowable limits in at least one single-objective optimization case. Since the TOPSIS method selects optimal solution closer to the minimum SIC point, the numerical values of the optimal decision variables are also closer to those obtained for minimum SIC case. It is also noted that number of tube passes in both condenser and evaporator decreases by transitioning from minimum SIC case to maximum second law efficiency case.

Table 8 reports the decision variables of the single-objective case and the multi-objective case for the basic ORC employing R245fa as a working fluid. It can be seen from the Table 8 that inclinations of the decision variables are very similar with those obtained for the cycle running with R236ea. However, TOPSIS solution resulted from multi objective optimization is more preferrable than that is obtained

Table 5 Upper and lower bounds of design variables for the basic ORC

Decision variables	Lower bound	Upper bound
Condenser outlet temperature (K)	303.15	313.15
Evaporator pressure (kPa)	85%–90% of the critical temperature	
Superheat temperature (K)	0.0	30.0
Evaporator pinch point temperature difference (K)	8.0	20.0
Condenser pinch point temperature difference (K)	5.0	15.0
Condenser outer tube diameter (m)	0.015	0.020
Condenser shell diamater (m)	0.25	0.50
Condenser baffling space (m)	0.15	0.50
Number of tube passes in the condenser	1–2–4-6-8	
Arrangement of the tubes in the condenser	Square-Triangle	
Evaporator outer tube diameter (m)	0.015	0.020
Evaporator shell diamater (m)	0.25	0.50
Evaporator baffling space (m)	0.15	0.50
Number of tube passes in the evaporator	1–2–4-6-8	
Arrangement of the tubes in the evaporator	Square-Triangle	
Mass flow rate of the refrigerant (kg/s)	0.1	0.8

for the system operated with R236ea as SIC and second law efficiency of the the cycle running with R245fa are respectively 4.1% lower and 3.3% higher than those correspondingly obtained for the cycle running with R236ea. The minimum SIC value of R245fa ORC is 5731.318 *$/kW* and its corresponding second law efficiency is 0.379, which are respectively 4.4% lower and 1.2% higher than those acquired by R236ea ORC when SIC is minimized. The maximum second law efficiency value is 0.476 and the corresponding SIC value is 23,764.288 *$/kW*, which is about 25.2 and 313.4% higher than the minimum SIC case. In the case of second law efficiency maximization for R245fa ORC, it is seen that

Table 6 Upper and lower bounds of design variables for the single-stage ORC

Decision variables	Lower bound	Upper bound
Condenser outlet temperature (K)	303.15	313.15
Evaporator pressure (kPa)	85%–90% of the critical temperature	
Feed heater pressure (kPa)	79%–84% of the critical temperature	
Superheat temperature (K)	0.0	30.0
Evaporator pinch point temperature difference (K)	8.0	20.0
Condenser pinch point temperature difference (K)	5.0	15.0
Condenser outer tube diameter (m)	0.015	0.020
Condenser shell diamater (m)	0.25	0.50
Condenser baffling space (m)	0.15	0.50
Number of tube passes in the condenser	1–2–4-6-8	
Arrangement of the tubes in the condenser	Square-Triangle	
Evaporator outer tube diameter (m)	0.015	0.020
Evaporator shell diamater (m)	0.20	0.50
Evaporator baffling space (m)	0.15	0.50
Number of tube passes in the evaporator	1–2–4-6-8	
Arrangement of the tubes in the evaporator	Square-Triangle	
Feed heater outer tube diameter (m)	0.015	0.020
Feed heater shell diamater (m)	0.25	0.50
Feed heater baffling space (m)	0.15	0.50
Number of tube passes in the feed heater	1–2–4-6-8	
Arrangement of the tubes in the feed heater	Square-Triangle	
Mass flow rate of the refrigerant (kg/s)	0.1	0.7

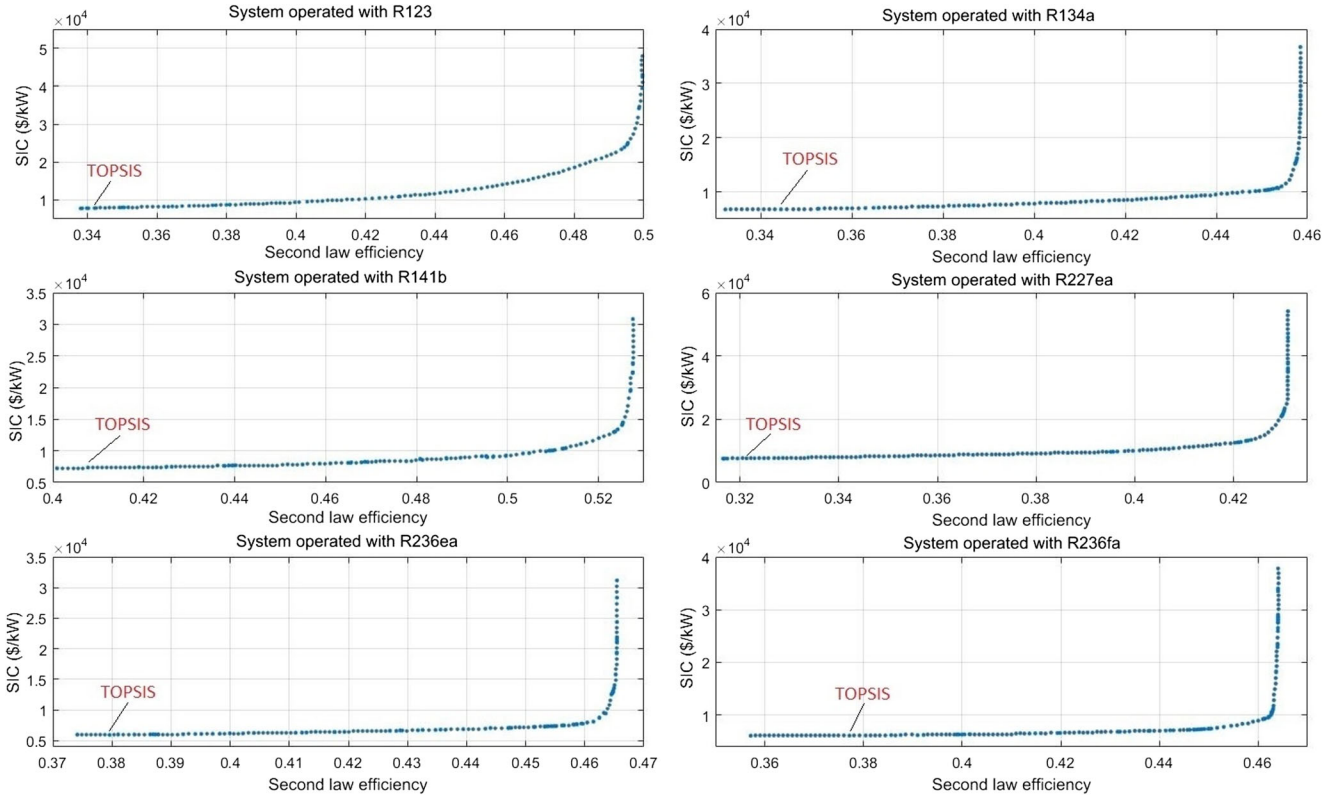

Fig. 4 Pareto optimal solutions of the first eight group of refrigerants for the basic ORC

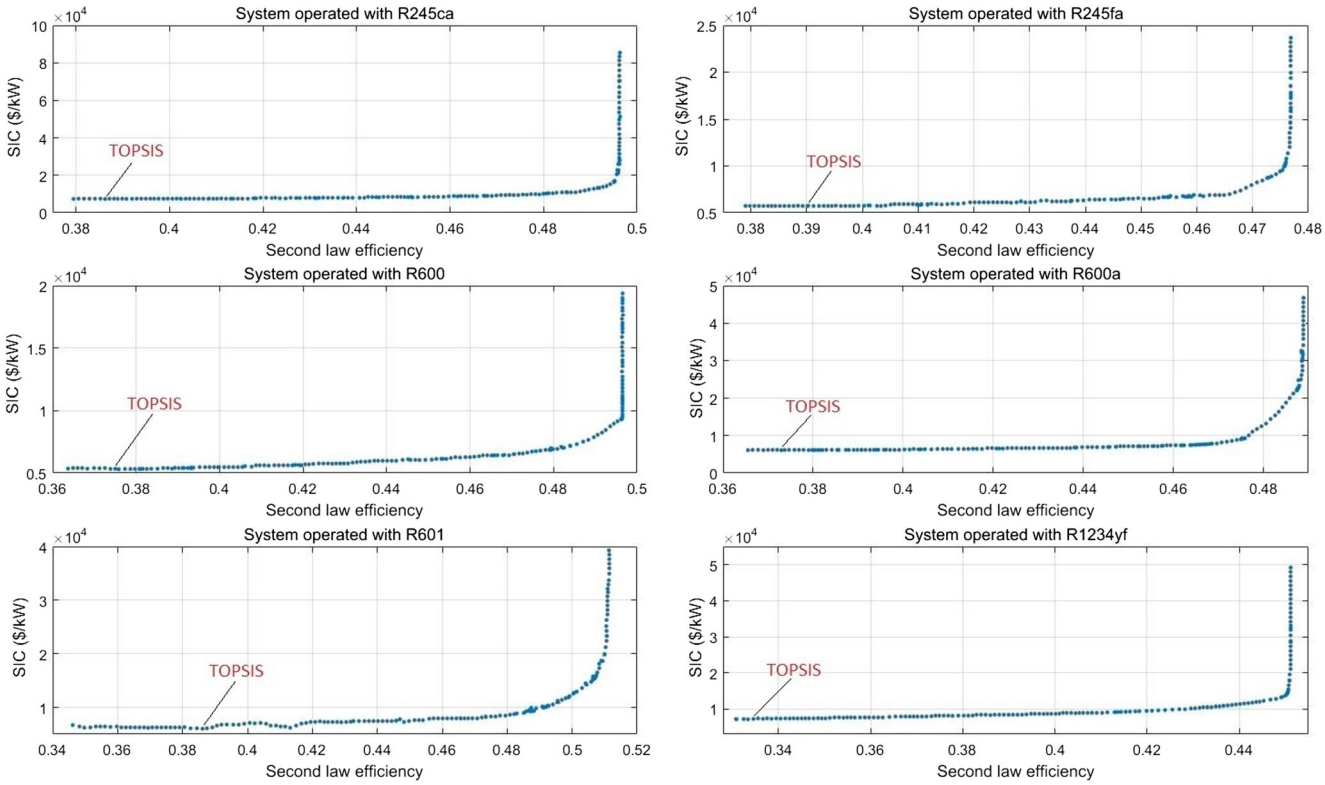

Fig. 5 Pareto optimal solutions of the second eight group of refrigerants for the basic ORC

Table 7 Single- and multi-objective optimization results of the basic ORC running with R236ea

	Minimum SIC	Maximum second law efficiency	TOPSIS
Condenser temperature (K)	303.153	303.145	303.150
Evaporator pressure (kPa)	2022.183	2826.561	2161.966
Superheat temperature (K)	2.772	20.853	0.387
Evaporator pinch point temperature difference (K)	15.686	8.000	12.341
Condenser pinch point temperature difference (K)	14.999	5.000	14.968
Condenser outer tube diameter (m)	0.015	0.015	0.015
Condenser shell diamater (m)	0.251	0.499	0.250
Condenser baffling space (m)	0.246	0.499	0.315
Number of tube passes in the condenser	4	1	4
Arrangement of the tubes in the condenser	Triangle	Square	Triangle
Evaporator outer tube diameter (m)	0.015	0.015	0.015
Evaporator shell diamater (m)	0.250	0.309	0.250
Evaporator baffling space (m)	0.150	0.499	0.150
Number of tube passes in the evaporator	8	1	8
Arrangement of the tubes in the evaporator	Square	Square	Square
Mass flow rate of the refrigerant (kg/s)	0.600	0.400	0.657
Second law efficiency	0.374	0.465	0.379
Specific Investment Cost ($/kW)	5988.496	31,185.805	5998.696

second law efficiency is increased by 24.9% (0.476) and SIC of the cycle is increased by 313% (23,764.288 *$/kW*) compared to the optimal objective function results obtained for minimum SIC case for the cycle working with the same refrigerant.

Table 9 reports the optimal values of the decision variables for the single-objective and multi-objective optimization cases for the basic ORC with R600 as working fluid. Tendencies of the decision variables of the R600 ORC are a bit different than those of the former mentioned cycles. Triangle tube

Table 8 Single- and multi-objective optimization results of the basic ORC working with R245fa

	Minimum SIC	Maximum second law efficiency	TOPSIS
Condenser temperature (K)	303.150	303.151	303.153
Evaporator pressure (kPa)	1429.719	1969.627	1546.195
Superheat temperature (K)	1.375	15.812	1.199
Evaporator pinch point temperature difference (K)	14.064	8.000	12.582
Condenser pinch point temperature difference (K)	14.997	5.000	14.892
Condenser outer tube diameter (m)	0.015	0.015	0.015
Condenser shell diamater (m)	0.250	0.499	0.250
Condenser baffling space (m)	0.314	0.499	0.358
Number of tube passes in the condenser	4	1	4
Arrangement of the tubes in the condenser	Square	Square	Triangle
Evaporator outer tube diameter (m)	0.015	0.015	0.015
Evaporator shell diamater (m)	0.251	0.320	0.251
Evaporator baffling space (m)	0.150	0.499	0.150
Number of tube passes in the evaporator	8	1	8
Arrangement of the tubes in the evaporator	Square	Square	Square
Mass flow rate of the refrigerant (kg/s)	0.533	0.400	0.521
Second law efficiency	0.379	0.476	0.390
Specific Investment Cost ($/kW)	5731.318	23,674.288	5783.423

Table 9 Single- and multi-objective optimization results of the basic ORC running with R600

	Minimum SIC	Maximum second law efficiency	TOPSIS
Condenser temperature (K)	303.202	303.263	303.150
Evaporator pressure (kPa)	1479.848	2100.410	1673.514
Superheat temperature (K)	6.379	19.921	0.060
Evaporator pinch point temperature difference (K)	14.216	8.014	14.856
Condenser pinch point temperature difference (K)	14.965	5.091	14.989
Condenser outer tube diameter (m)	0.015	0.015	0.015
Condenser shell diamater (m)	0.276	0.496	0.281
Condenser baffling space (m)	0.182	0.489	0.168
Number of tube passes in the condenser	6	2	6
Arrangement of the tubes in the condenser	Triangle	Triangle	Triangle
Evaporator outer tube diameter (m)	0.015	0.017	0.015
Evaporator shell diamater (m)	0.251	0.486	0.250
Evaporator baffling space (m)	0.157	0.485	0.150
Number of tube passes in the evaporator	8	1	8
Arrangement of the tubes in the evaporator	Triangle	Square	Triangle
Mass flow rate of the refrigerant (kg/s)	0.298	0.111	0.282
Second law efficiency	0.363	0.496	0.375
Specific Investment Cost ($/kW)	5351.095	19,378.383	5394.612

arrangement is dominant for condenser and evaporator for both optimization cases. The minimum SIC is 5351.095 *$/kW*, which is about 7.6% lower than that is obtained for R245fa ORC and 12.4% lower than that is found for R236ea ORC. Maximum second law efficiency is 0.363, which is 2.5% lower than that is obtained for R245fa ORC and 3.2% lower than that is obtained for R236ea ORC. The optimal solution chosen by TOPSIS method for R600 ORC is also given in Table 9. Optimal SIC value acquired by TOPSIS method is 5394.612 *$/kW*, which is 8.2% lower than that is found for R245fa ORC and 12.5% lower than that is obtained for R236ea ORC. Optimal second law efficiency value found by TOPSIS method is 0.375, which is 4.3% lower than that is found for R245fa ORC and 1.1% lower than that is found for R236ea ORC. Maximum second law efficiency is 0.496 and its corresponding SIC is 19,378.383 *$/kW*.

In all three best performer refrigerants cases of the basic ORC, convergence to the maximum or minimum limits of the same decision variables can be observed. The condenser outlet temperature hit the minimum limit for all three cases. This behaviour can be explained by thermophysical characteristics of the refrigerants in lower temperatures give rise to higher cycle efficiencies and lower costs. Another important point that is worth to mention that outer tube diameters of the heat exchangers converge to minimum allowable limits for all cases. This can be explained by the fact that lower tube diameters increase the convective heat transfer coefficient of the inner flow, therefore, heat transfer between the fluids in the heat exchangers increases which causes a more efficient thermodynamic cycle configuration with a lower incurred total cost. Also, the superheat temperatures are lower for the minimum SIC cases than second law efficiency cases. The superheat temperatures of the minimum SIC cases are %13.2, %8.6 and %32 of the maximum second law efficiency cases for the R236ea, R245fa and R600 refrigerants respectively. Moreover, it has been found out that among the best performers, R600 has the lowest minimum SIC value while R236ea has the highest maximum second law efficiency value for the basic ORC case studies.

Figures 6 and 7 show the Pareto optimal solutions of the single-stage ORC working with different refrigerants. Same as the basic ORC cases, corresponding optimal SIC, second law efficiency and decision variables of the points with the maximum second law efficiency, minimum SIC and the optimal point selected by the TOPSIS method are respectively given in Tables 10, 11 and 12. It can be seen from the Pareto curves that some refrigerants such as R245fa and R134a are not very efficient in the basic ORC and their corresponding thermal performance are much better in the single stage ORC. The main reason behind this performance increase is the result of having more suitable thermodynamic characteristics for being reprocessed in higher pressures. The top three performing refrigerants of the single-stage ORC are R245ca, R245fa and R600. Table 10 reports the decision variables of the single- and multi-objective optimization solutions of single-stage ORC employing R245ca as process fluid. Optimal SIC and second law efficiency of R245ca chosen by TOPSIS method are correspondingly 6785.109 *$/kW* and 0.407. Inclinations of

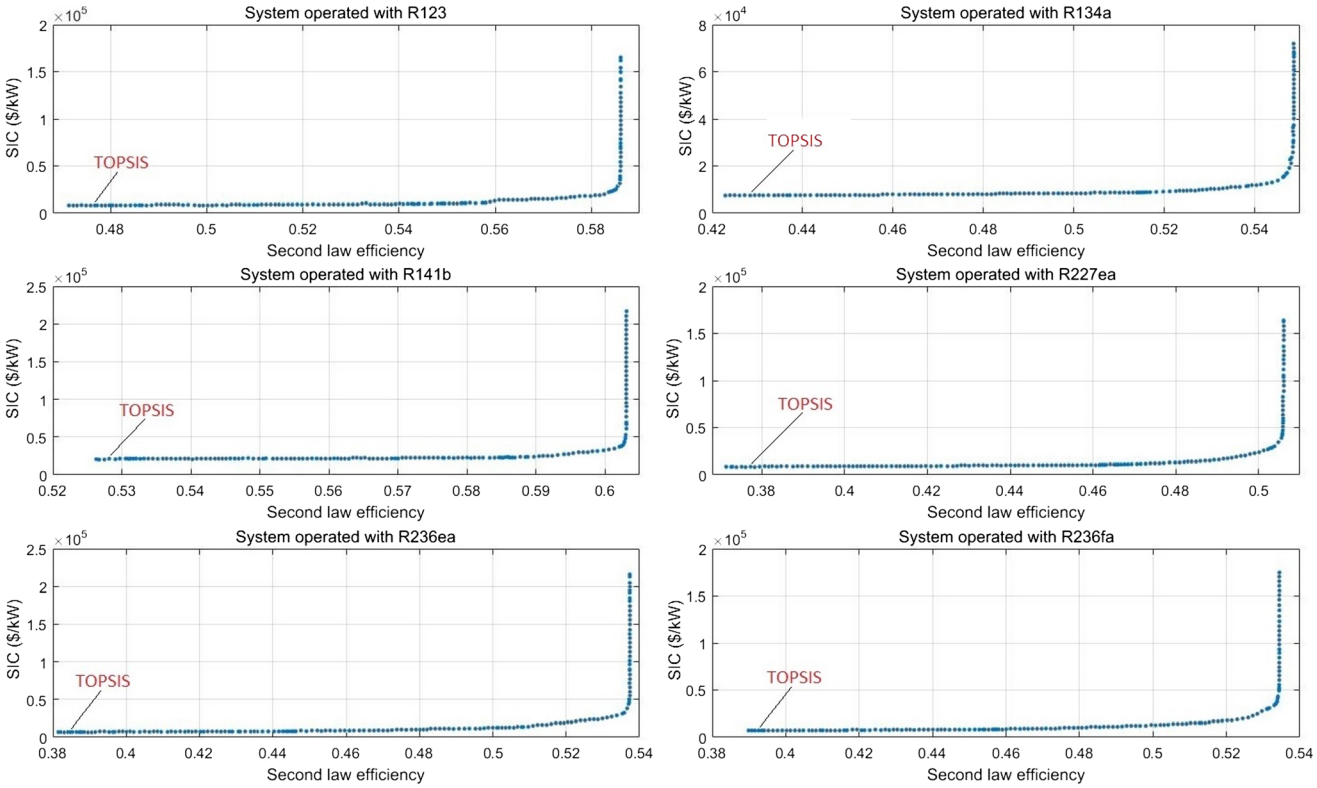

Fig. 6 Pareto optimal solutions of the first eight group of the refrigerants for the single-stage ORC

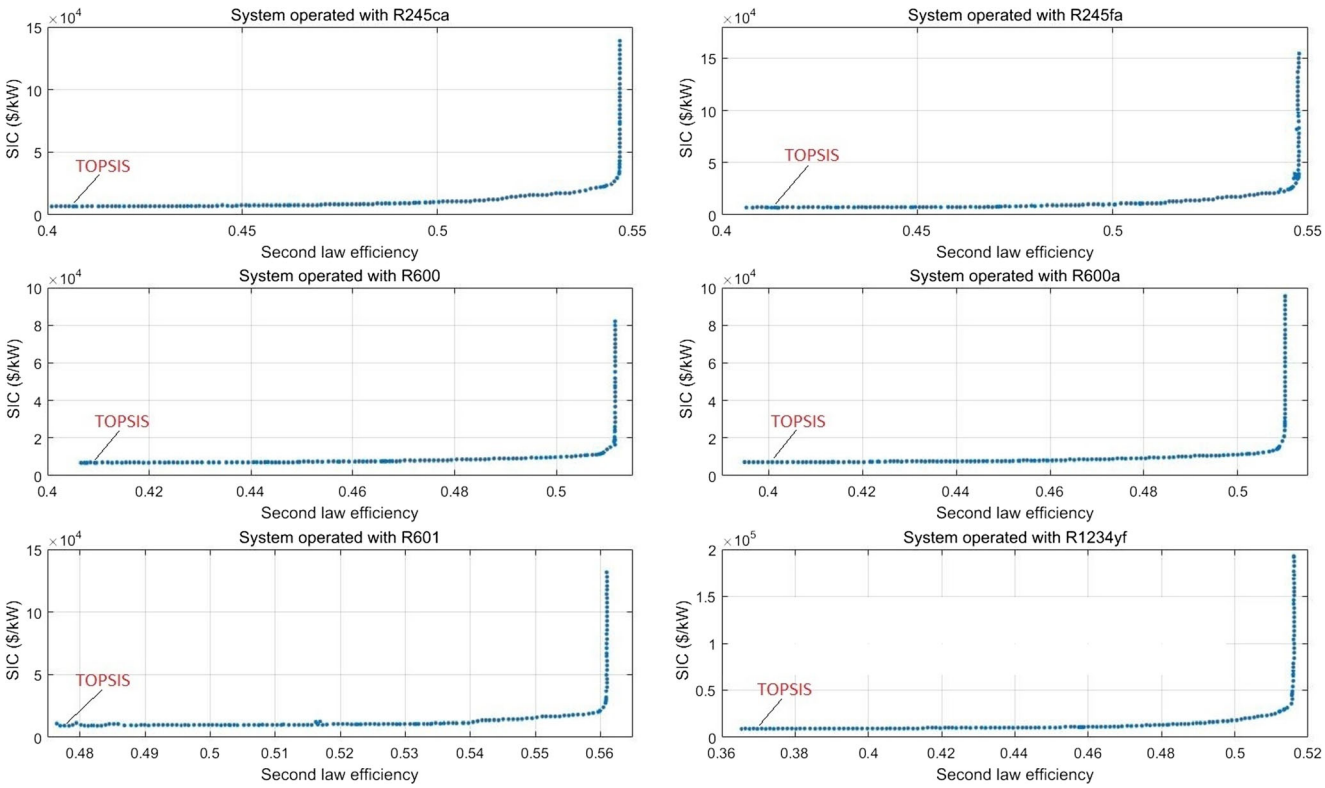

Fig. 7 Pareto optimal solutions of the second eight group of the refrigerants for the single-stage ORC

Table 10 Single- and multi-objective optimization results of the single-stage ORC employing R245ca

	Minimum SIC	Maximum second law efficiency	TOPSIS
Condenser temperature (K)	303.152	303.150	303.150
Evaporator pressure (kPa)	917.409	930.792	930.386
Feed heater pressure (kPa)	282.177	394.458	282.254
Superheat temperature (K)	18.829	2.256	14.852
Evaporator pinch point temperature difference (K)	12.904	8.000	10.448
Condenser pinch point temperature difference (K)	14.991	5.000	14.949
Condenser outer tube diameter (m)	0.019	0.019	0.019
Condenser shell diamater (m)	0.251	0.499	0.252
Condenser baffling space (m)	0.150	0.211	0.151
Number of tube passes in the condenser	4	1	4
Arrangement of the tubes in the condenser	Triangle	Triangle	Triangle
Evaporator outer tube diameter (m)	0.015	0.015	0.015
Evaporator shell diamater (m)	0.217	0.400	0.227
Evaporator baffling space (m)	0.150	0.499	0.150
Number of tube passes in the evaporator	6	2	6
Arrangement of the tubes in the evaporator	Square	Square	Square
Feed heater outer tube diameter (m)	0.015	0.015	0.015
Feed heater shell diamater (m)	0.250	0.499	0.250
Feed heater baffling space (m)	0.150	0.481	0.150
Number of tube passes in the feed heater	8	1	8
Arrangement of the tubes in the feed heater	Square	Triangle	Square
Mass flow rate of the refrigerant (kg/s)	0.471	0.200	0.503
Second law efficiency	0.401	0.546	0.407
Specific Investment Cost ($/kW)	6756.924	138,868.776	6785.109

the decision variables for single stage ORCs are similar with those obtained for basic ORC working above discussed refrigerants. Triangle type tube arrangement is prevalent in the condenser while tube arrangement of evaporator is square for both design optimization cases. Evaporator working pressure is much lower than those of the above compared refrigerants, which is the result of thermodynamic characteristic of R245ca itself. Optimal superheat temperatures are decreased from 18.829 to 2.256 when optimization objectives are shifted from SIC to second law efficiency. Optimal values of number of tube pass in condenser and evaporator are inclined to their allowed upper bound when SIC is minimized, however these design variables are tend to get their minimum values when second law efficiency is maximized. In addition, it is observed that inclinations of design variables of feed header is similar with those of the evaporator. Single-objective minimization result of SIC value is 6756.924 *$/kW* and its corresponding second law efficiency is 0.401, whereas single objective maximization result of second law efficiency is 0.546 and its respective SIC is 138,868.776 *$/kW* for the single stage ORC working with R245ca.

Table 11 reports the optimal results of the decision variables for the single-objective and multi-objective design optimization for single-stage R245fa ORC. Again, similar tendencies of the decision variables with single-stage R245ca case and basic cycle R245fa can be observed. Minimum SIC value and maximum second law efficiency are respectively increased by 21.7 and 14.9% compared to basic ORC in the case of single objective optimization. Marked decreases are seen in evaporator pressures for minimum SIC and maximum second law effficiency cases in comparison with basic ORC design. Optimal values of condenser baffle spacing when SIC is minimized and second law efficiency is maximized are respectively decreased by 48.3 and 37.2% when single-stage ORC design is considered instead of basic ORC. TOPSIS result of single stage R245fa ORC for the second law efficiency and the SIC are respectively increased by 6.3 and 21.1% compared to those obtained for R245fa basic ORC. Table 12 reports optimal design variables for the single-objective and multi-objective optimization of the single-stage ORC employing R600 as working fluid. Optimal value for the individual optimization of SIC for this case is 25.9% higher than that is found for basic R600 ORC. In addition, there occurs an increase in optimal second law efficiency by 11.8% compared to that is obtained for basic R600 ORC. There is also an evident increase in second law efficiency (9.7%) and

Table 11 Single- and multi-objective optimization results of the single-stage ORC operated with R245fa

	Minimum SIC	Maximum second law efficiency	TOPSIS
Condenser temperature (K)	303.182	303.150	303.166
Evaporator pressure (kPa)	1242.937	1264.579	1263.184
Feed heater pressure (kPa)	514.751	583.648	456.757
Superheat temperature (K)	18.899	1.568	24.534
Evaporator pinch point temperature difference (K)	13.289	8.000	11.084
Condenser pinch point temperature difference (K)	14.928	5.000	14.516
Condenser outer tube diameter (m)	0.019	0.019	0.199
Condenser shell diamater (m)	0.251	0.497	0.250
Condenser baffling space (m)	0.150	0.188	0.151
Number of tube passes in the condenser	4	1	4
Arrangement of the tubes in the condenser	Triangle	Triangle	Triangle
Evaporator outer tube diameter (m)	0.015	0.015	0.015
Evaporator shell diamater (m)	0.200	0.403	0.200
Evaporator baffling space (m)	0.151	0.499	0.150
Number of tube passes in the evaporator	6	2	6
Arrangement of the tubes in the evaporator	Triangle	Square	Triangle
Feed heater outer tube diameter (m)	0.015	0.015	0.015
Feed heater shell diamater (m)	0.253	0.488	0.250
Feed heater baffling space (m)	0.150	0.397	0.155
Number of tube passes in the feed heater	8	1	8
Arrangement of the tubes in the feed heater	Square	Triangle	Square
Mass flow rate of the refrigerant (kg/s)	0.521	0.200	0.519
Second law efficiency	0.407	0.547	0.414
Specific Investment Cost ($/kW)	6979.749	154,371.322	6999.496

SIC(25.7%) for TOPSIS results compared to those found for the basic R600 ORC. These increases in specific investment cost values are mainly due to the additional cost burdened by the integration of feed heaters to the ORC. Similar inclinations are observed in design variables for the basic and single stage R600 ORC. A notable phenomenon for all of the optimization cases is that the heat exchanger pinch point temperatures hit the minimum allowable limits for the maximum second law efficiency cases. This inclination can be explained by the lower temperature differences between the hot and cold mediums and process fluid, which causes a recognizable reduction in entropy generation rates leading to higher second law efficiency values. Moreover, unlike the basic ORC cases, higher superheat temperature leads to more desirable SIC performance. The superheat temperatures for the maximum second law efficiency cases are %11.9, %8.2 and %17.37 of the minimum SIC cases for the R245ca, R245fa and R600 refrigerants respectively.

Table 13 reports the single-objective optimization results of the basic and single-stage ORCs discussed in this study. It can be seen from the table that R123 ORC has the maximum SIC value (7763.154 *$/kW*) when SIC is individually minimized for basic ORC. Its corresponding second law efficiency is 0.337. One can conclude that R123 ORC gives one of the worst cycle performances with respect to numerical values of the objective functions when only SIC is minimized. As mentioned in above paragraphs, minimum SIC is attained by R600 ORC (5351.095 *$/kW*) and its respective second law efficiency is 0.363, which both results are superior to the most of the results those found for the refrigerant-cycle pairs when SIC is minimized for the basic ORC. When second law efficiency is optimized for basic ORC, R141 gives the best performance with having second law efficiency of the cycle of 0.527. It is closely followed by R601 with having objective function value of 0.511. The worst performance is given by the R227ea ORC with having optimal second law efficiency of 0.431 when this design objective is maximized for basic ORC. Through examining the optimal solutions of the single stage ORC, one can say that there is an increase in both objective function values. As mentioned above, increase in SIC values is the result of additional cost incurred by the integration of feed heater to the cycle, however utilization of feed

Table 12 Single- and multi-objective optimization results of the single-stage ORC working with R600

	Minimum SIC	Maximum second law efficiency	TOPSIS
Condenser outlet temperature (K)	303.151	303.150	303.167
Evaporator pressure (kPa)	1494.098	1525.875	1512.109
Feed heater pressure (kPa)	563.685	754.618	565.246
Superheat temperature (K)	20.631	3.584	22.544
Evaporator pinch point temperature difference (K)	9.361	8.000	9.565
Condenser pinch point temperature difference (K)	14.999	5.000	14.988
Condenser outer tube diameter (m)	0.019	0.019	0.019
Condenser shell diamater (m)	0.250	0.499	0.250
Condenser baffling space (m)	0.150	0.161	0.150
Number of tube passes in the condenser	4	1	4
Arrangement of the tubes in the condenser	Square	Triangle	Triangle
Evaporator outer tube diameter (m)	0.015	0.015	0.015
Evaporator shell diamater (m)	0.200	0.499	0.200
Evaporator baffling space (m)	0.150	0.499	0.150
Number of tube passes in the evaporator	6	2	6
Arrangement of the tubes in the evaporator	Square	Square	Square
Feed heater outer tube diameter (m)	0.015	0.015	0.015
Feed heater shell diamater (m)	0.250	0.498	0.250
Feed heater baffling space (m)	0.150	0.497	0.150
Number of tube passes in the feed heater	8	1	8
Arrangement of the tubes in the feed heater	Square	Triangle	Square
Mass flow rate of the refrigerant (kg/s)	0.291	0.200	0.283
Second law efficiency	0.406	0.511	0.409
Specific Investment Cost ($/kW)	6737.327	82,002.349	6792.412

Table 13 Single-objective optimization results of the basic and single-stage ORCs

	Basic ORC				Single-stage ORC			
	SIC minimum case		Sec. law eff. Max. case		SIC minimum case		Sec. law eff. Max. case	
Refrigerant	SIC	Sec. law eff.	SIC	Sec. law eff.	SIC	Sec. law eff.	SIC	Sec. law eff.
R123	7763.154	0.337	47,902.022	0.499	8311.922	0.477	165,163.568	0.586
R134a	6738.720	0.332	36,692.916	0.458	7412.773	0.422	67,908.076	0.541
R141b	7230.697	0.400	30,830.363	0.527	19,773.454	0.526	216,794.664	0.603
R227ea	7529.457	0.316	54,137.679	0.431	8597.206	0.371	163,561.234	0.506
R236ea	5988.496	0.374	31,185.805	0.465	7028.892	0.381	215,936.536	0.537
R236fa	6115.025	0.357	37,834.071	0.464	7227.016	0.390	174,678.804	0.534
R245ca	7333.371	0.379	85,399.259	0.496	6756.924	0.401	138,868.776	0.546
R245fa	5731.318	0.379	23,674.288	0.476	6979.749	0.407	154,371.322	0.547
R600	5351.095	0.363	19,378.383	0.496	6737.327	0.406	82,002.349	0.511
R600a	6132.732	0.373	46,722.660	0.488	7163.319	0.394	95,517.775	0.510
R601	6688.454	0.346	39,300.525	0.511	9274.676	0.476	131,593.100	0.560
R1234yf	7195.788	0.330	49,232.176	0.451	8926.706	0.365	192,674.895	0.516

heater in the cycle results in a considerable increase in second law efficiency rates. Feed heater allows reutilization of the process fluid with having high grade energy in the turbine, which correspondingly entails an increase in first and second law efficiencies of the thermodynamic cycle. Best optimal SIC value for single stage ORC is obtained by the cycle working with R600 (6737.327 $/kW), and closely followed by the cycle running with R245ca (6756.924 $/kW). Corresponding second law efficiency values are respectively 0.406 for R600 single-stage ORC and 0.496 for R245ca SSORC when SIC is minimized for single stage ORC. Maximum SIC value is obtained by R141b single-stage ORC (19,773.454 $/kW), which is nearly higher than twice of that obtained by the second worst refrigerant-cyle pair R601 single-stage ORC (9274.676 $/kW) in the case of minimization of SIC for the single stage ORC. Best performance is given by R141b SSORC with having second law efficiency of 0.603 when individual optimization of the objective function of second law efficiency is maintained. Second best performing refrigerant cycle pair is R123 single-stage ORC with having optimized second law efficiency of 0.586. R227ea SSORC shows the worst performance with having second law efficiency of 0.506. Tables 14 and 15 report the state temperatures at each point in the basic and single-stage ORCs obtained for TOPSIS results of the three best performing refrigerants. Moreover, among the best performer refrigerants of the single-stage ORC case, it has been found out that R600 has the lowest minimum SIC value and R245fa has the maximum second law efficiency value.

4.2 Sensitivity analysis

By taking the optimal solution selected by the TOPSIS method as a pivot point, the effect of variation of the each decision variable to the two main objective function used in this paper, the SIC and the second law efficiency, is studied for the best performing refrigerants for both basic and single-stage ORCs.

Table 14 Thermal conditions of the each point in the basic ORC that employs the best performing three refrigerants based on the optimal solution chosen by the TOPSIS method

State (K)	R236ea	R245fa	R600
1	304.258	303.903	304.112
2	388.896	383.593	378.005
3	329.305	327.034	324.424
4	303.150	303.153	303.150
5	429.985	429.989	429.994
6	358.952	362.559	361.541
7	282.161	282.391	282.151
8	288.856	288.703	288.580

Table 15 Thermal conditions of the each point in the single-stage ORC that employs the best performing three refrigerants based on the optimal solution chosen by the TOPSIS method

State (K)	R245ca	R245fa	R600
1	303.225	303.320	303.363
2	328.168	332.715	328.262
3	328.523	333.262	329.038
4	387.983	397.624	395.230
5	360.301	370.933	365.815
6	344.104	351.103	348.976
7	303.150	303.166	303.167
8	429.978	429.921	429.997
9	365.062	367.131	362.815
10	282.966	283.747	282.954
11	289.008	289.622	289.229

R600 is selected as the best performing refrigerant for the basic ORC because of its favorable optimal SIC performance. Figure 8a and b show the sensitivity analysis of a basic ORC with R600 refrigerant. It can be seen from the Fig. 8a that the evaporator pressure has a big influence on the second law efficiency and the SIC of the cycle. Controversial effects of the arrangement of the tubes in the heat exchangers on the objectives can be noted. Variation of the pinch point temperatures in the heat exchangers have similar effects on the SIC and second law efficiency of the cycle. Also, one can see the importance of the evaporator shell diameter, number of tube passes in the evaporator and mass flow rate of the refrigerant on the problem objectives. Variation of the condenser outlet temperature and evaporator pressure has an opposite influence on the objectives. Furthermore, decrease of the refrigerant mass flow rate reduces the nmerical value of both objectives.

R600 still shows better performance than the other refrigerants in terms of SIC for the single-stage ORC, however, with the intention of analyzing the tendencies of a different refrigerant, R245fa is selected because of its superior second law efficiency performance. Figure 9a, b and c show the sensitivity analysis of a single-stage ORC with R245fa refrigerant. Decrease of the feed heater outer tube diameter takes the SIC value down and the second law efficiency value up. This inclination explains the tendency of the feed heater outer tube diameter decision variable hitting minimum in the optimization cases. Similar to the basic ORC case, decrease of the refrigerant mass flow rate reduces the values of the both objectives. Controversial effects of the condenser outlet temperature and the evaporator pressure on the objectives can be noted. Triangular arrangement of the tubes in the evaporator and the feed heater increases the values of the both objectives, on the other hand, takes the

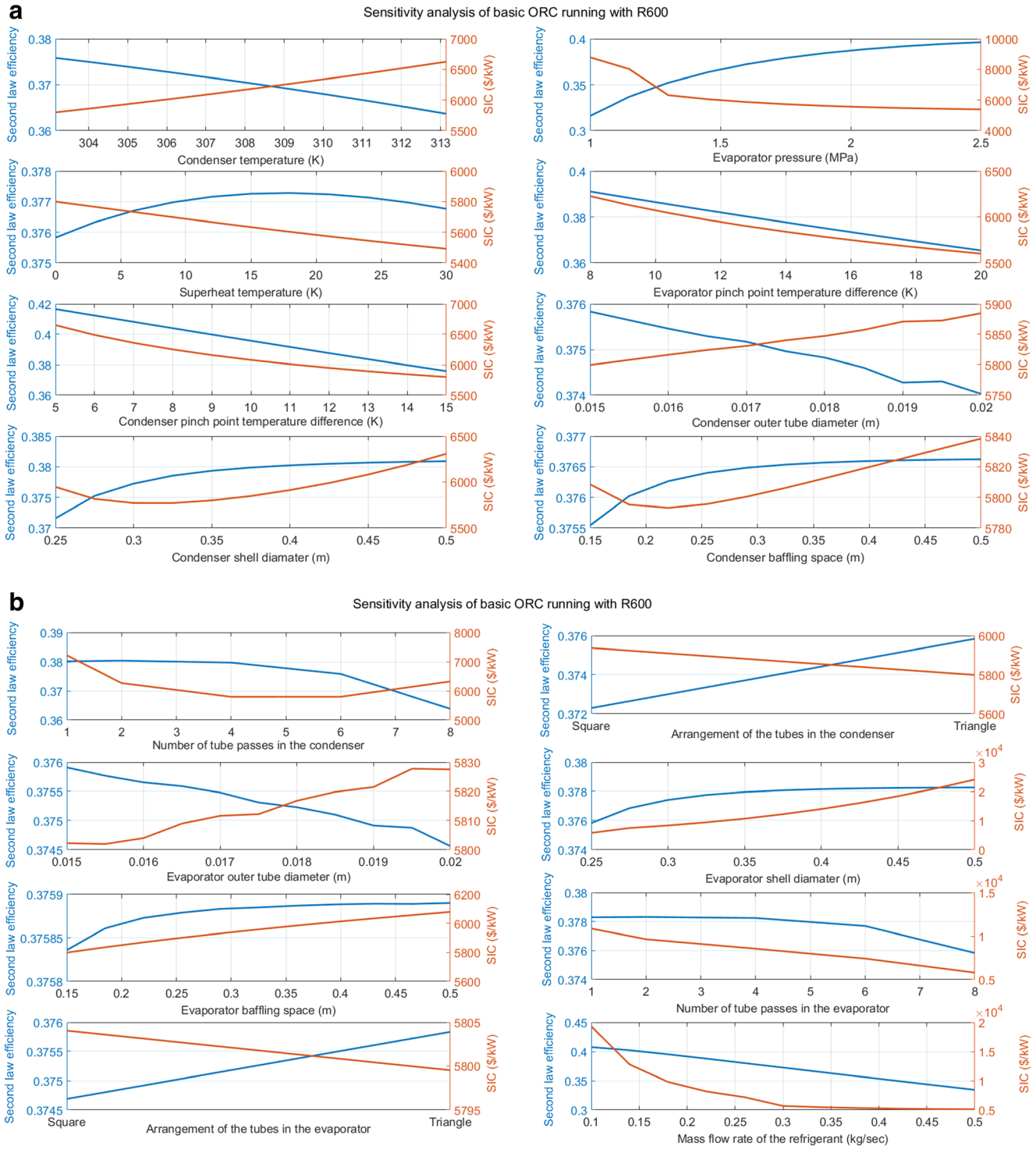

Fig. 8 **a** Sensitivity analysis of the first eight decision variables for the basic ORC employing R600. **b** Sensitivity analysis of the second eight decision variables for the basic ORC employing R600

value of the SIC down while increase the value of the second law efficiency in the condenser. Also, it is worth to mention that the second law efficiency reaches to its maximum value when the feed heater pressure is around 0.55 MPa.

5 Conclusion

This paper deals with the multi-objective optimization of the basic and single-stage ORC systems operated with twelve different refrigerants by considering a low-grade heat source.

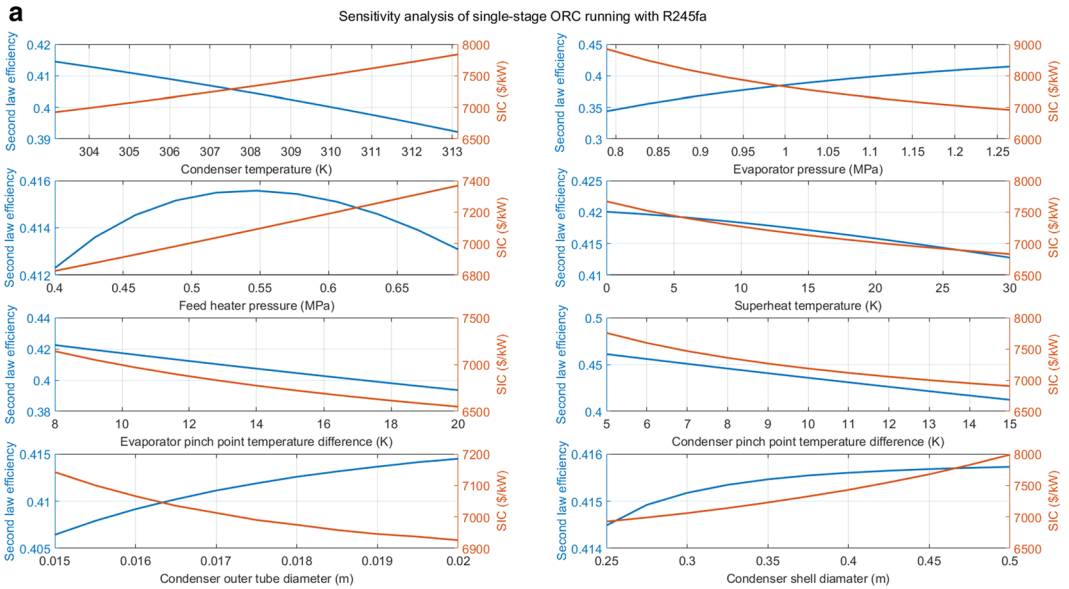
a
Sensitivity analysis of single-stage ORC running with R245fa
Second law efficiency
SIC ($/kW)
Condenser temperature (K)
Evaporator pressure (MPa)
Feed heater pressure (MPa)
Superheat temperature (K)
Evaporator pinch point temperature difference (K)
Condenser pinch point temperature difference (K)
Condenser outer tube diameter (m)
Condenser shell diamater (m)

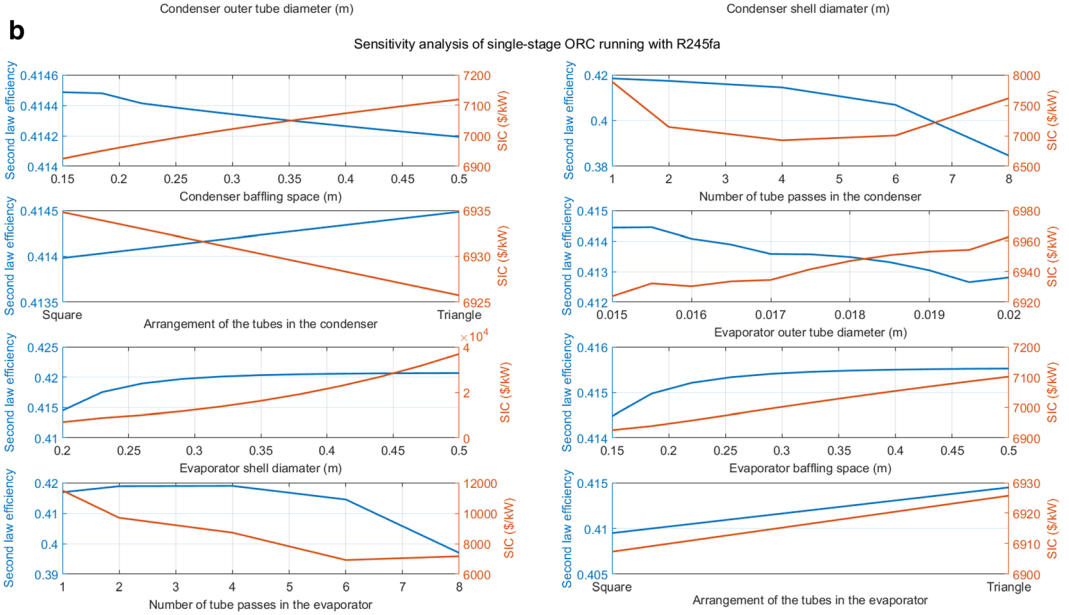
b
Sensitivity analysis of single-stage ORC running with R245fa
Second law efficiency
SIC ($/kW)
Condenser baffling space (m)
Number of tube passes in the condenser
Square
Triangle
Arrangement of the tubes in the condenser
Evaporator outer tube diameter (m)
Evaporator shell diamater (m)
Evaporator baffling space (m)
Number of tube passes in the evaporator
Arrangement of the tubes in the evaporator

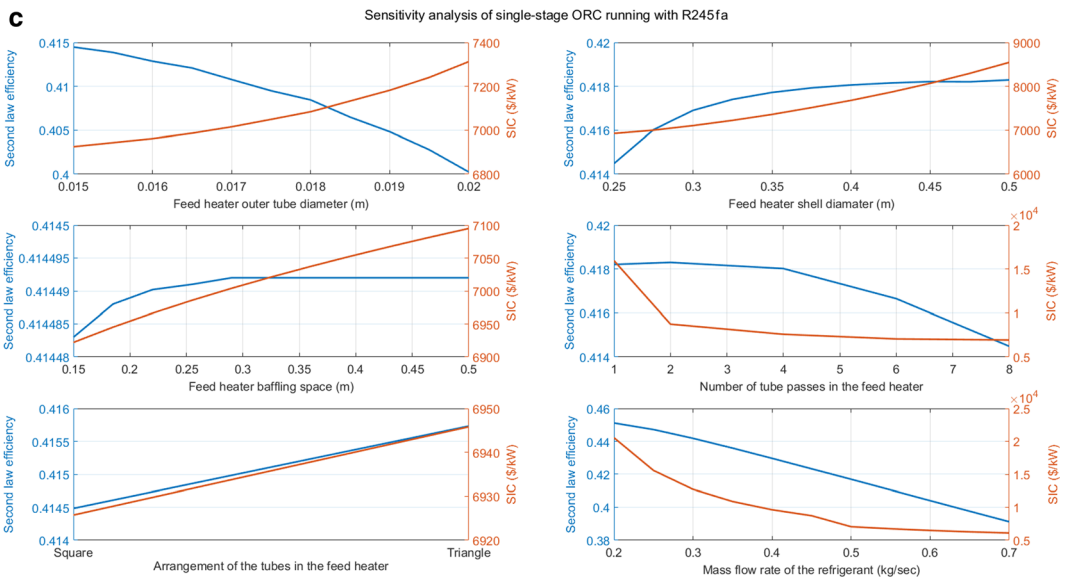
c
Sensitivity analysis of single-stage ORC running with R245fa
Second law efficiency
SIC ($/kW)
Feed heater outer tube diameter (m)
Feed heater shell diamater (m)
Feed heater baffling space (m)
Number of tube passes in the feed heater
Square
Triangle
Arrangement of the tubes in the feed heater
Mass flow rate of the refrigerant (kg/sec)

◀ **Fig. 9** **a** Sensitivity analysis of the first eight decision variables for the single-stage ORC employing R245fa. **b** Sensitivity analysis of the second eight decision variables for the single-stage ORC employing R245fa. **c** Sensitivity analysis of the last six decision variables for the single-stage ORC employing R245fa

The maximum temperature of the heat source is considered as 430.15 *K*. The group of refrigerants to be compared in terms of cycle efficiency include isentropic and dry fluids as wet fluids require an extra superheat at the turbine inlet to protect the turbine blades from the liquid droplets which ultimately jeopardizes the thermal efficiency of the cycle. Modeling of the multi-objective ORC optimization problem is accomplished with sixteen decision variables for the basic cycle and twenty two decision variables for the single-stage cycle. The decision variables of the basic cycle include the condenser temperature, evaporator pressure, temperature difference with the heat source and the refrigerant at the pinch point of the condenser and the evaporator, mass flow rate of the refrigerant and some design parameters concerning the heat exchange components of the cycle. Two design objectives including Specific Investment Cost (SIC) and the second law efficiency of the cycle are considered for the multi-objective optimization problem. These two objectives are concurrently and seperately optimized and the results of the refrigerant-cycle pairs are compared with each other. Different from the other studies in the literature that deals with the design optimization of the ORCs, this study deals with more in-depth design variables, such as design configuration of the heat exchangers, with taking into account two conflicting objectives and various working fluids. The optimization task is handled by the Artificial Cooperative Search algorithm. By utilizing the merits of ACS algorithm, Pareto curve of the each refrigerant-cycle pair is generated and the best solution in the Pareto curve is chosen by the TOPSIS multi-criteria decision-making method. It is observed that the TOPSIS method selects the optimum solution that are closer to the minimum SIC solution rather than the optimum solution regarding maximum second law efficiency. Three best performing refrigerants are selected from each basic and single-stage ORC and the numerical outcomes of the thermodynamic cycles with using these refrigerants are compared with each other. R236ea, R245fa and R600 are selected as the best performers of the basic ORC and R245ca, R245fa and R600 are selected as the best performers of the single-stage ORC. All three best performer refrigerants of the each cycle are non-dominant to each other and have favorable SIC and second law efficiency characteristics. A sensitivity analysis is performed for each best performing refrigerant-cycle pair to observe the impact of each decision variable on the problem objectives. R600 is selected for the sensitivity analysis of the basic ORC due to its desirable optimal SIC performance. Moreover, R245fa is chosen for the sensitivity analysis of the single-stage ORC because of its favorable optimal second law efficiency performance. It is observed from the sensitivity analysis that the evaporator shell diameter, number of tube passes in the evaporator, evaporator pressure and mass flow rate of the refrigerant are the decision variable that has the highest influence on the considered problem objectives.

Compliance with ethical Standarts

Conflict of interest On behalf of all authors, the corresponding author states that there is no conflict of interest.

Ethical approval This article does not contain any studies with human participants or animals performed by any of the authors.

Informed consent Informed consent was obtained from all individual participants included in the study.

Publisher's Note Springer Nature remains neutral with regard to jurisdictional claims in published maps and institutional affiliations.

References

1. Andreasen JG, Larsen U, Knudsen T, Pierobon L, Haglind F (2013) Selection and optimization of pure and mixed working fluids for low grade heat utilization using organic Rankine cycles. Energy 73: 204–213
2. Macchi E, Astolfi M (2016) Organic Rankine Cycle (ORC) Power Systems. Technologies and Applications. Woodhead Publishing
3. Rahbar K, Mahmoud S, Al-Dadah RK, Moazami N, Mirhadizadeh SA (2017) Review of organic Rankine cycle for small-scale applications. Energy Convers Manag 134:135–155
4. Aboelwafa O, Fateen S-EK, Soliman A, Ismail IM (2018) A review on solar Rankine cycles: working fluids, applications, and cycle modifications. Renew Sust Energy Rev 82:868–885
5. Desai NB, Bandyophadhyay S (2016) Thermo-economic analysis and selection of working fluid for solar organic Rankine cycle. Appl Therm Eng 95:471–481
6. Bao J, Zhao L (2013) A review of working fluid and expander selections for organic Rankine cycle. Renew Sust Energy Rev 24: 325–342
7. Xi H, Li M-J, Xu C, He Y-L (2013) Parametric optimization of regenerative organic Rankine cycle (ORC) for low grade waste heat recovery using genetic algorithm. Energy 58:473–482
8. Hayat N, Ameen MT, Tariq MK, Shah SNA, Naveed A (2017) Dual-objective optimization of organic Rankine cycle (ORC) systems using genetic algorithm: a comparison between basic and recuperative cycles. Heat Mass Transf 53:2577–2596
9. Yilmaz F, Selbas R, Sahin AS (2016) Efficiency analysis of organic Rankine cycle with internal heat exchanger using neural network. Heat Mass Transf 52:351–359
10. Pierobon L, Nguyen T-V, Larsen U, Haglind F, Elmegaard B (2013) Multi-objective optimization of organic Rankine cycles for waste heat recovery: application in an offshore platform. Energy 58:538–549
11. Kazemi N, Samedi F (2016) Thermodynamic, economic and thermo-economic optimization of a new proposed organic Rankine cycle for energy production from geothermal sources. Energy Convers Manag 121:391–401
12. Yang M-H, Yeh R-H (2016) Economic performances optimization of an organic Rankine cycle system with lower global warming potential working fluids in geothermal application. Renew Energ 85:1201–1213

13. Khaljani M, Saray RK, Bahlouli K (2015) Thermodynamic and thermoeconomic optimization of an integrated gas turbine and organic Rankine cycle. Energy 93:2136–2145
14. Imran M, Park BS, Kim HJ, Lee DH, Usman M, Heo M (2014) Thermo-economic optimization of regenerative organic Rankine cycle for waste heat recovery applications. Energy Convers Manag 87:107–118
15. Civicioglu P (2013) Artificial cooperative search algorithm for numerical optimization problems. J Inf Sci 229:58–76
16. Li Y-R, Du M-T, Wu C-M, Wu S-Y, Liu C (2014) Potential of organic Rankine cycle using zeotropic mixtures working fluids for waste heat recovery. Energy 77:509–519
17. Bell IH, Wronski J, Quoilin S, Lemort V (2014) Pure and pseudo-pure fluid Thermophysical property evaluation and the open-source Thermophysical property library CoolProp. Ind Eng Chem Res 53: 2498–2508
18. Li M, Wang J, Li S, Wang X, He W, Dai Y (2014) Thermo-economic analysis and comparison of a CO_2 transcritical power cycle and an organic Rankine cycle. Geothermics 50:101–111
19. Sinnot RK (2009) Chemical Engineering Design, Butterworth-Heinemann
20. Gnielinski V (1976) New equations for heat and mass transfer in turbulent pipe and channel flow. Int Chem Eng 16:359–367
21. Florides GA, Kalogirou SA, Tassou SA, Wrobel LC (2003) Design and construction of LiBr-water absorption machine. Energ Convers Manage 44:2483–2508
22. Jakob M (1962) Heat transfer, 8th edn. John Wiley & Sons, New York, USA
23. Gungor KE, Winterton RHS (1986) A general correlation for flow boiling in tubes and annuli. Int J Heat Mass Transf 29:351–358
24. Safarian S, Aramoun F (2015) Energy and exergy assessments of modified organic Rankine cycles (ORCs). Energy Reports 1:1–7
25. Deb K (2014) Multi-objective optimization. in:Search Methodologies Introductory Tutorials in Optimization and Decision Support Techniques, eds. Edmund K. Burke and Graham Kendall, 2nd edition, Springer, New York USA
26. Kumar R, Kaushik SC, Kumar R, Hans R (2016) Multi-objective thermodynamic optimization of an irreversible regenerative Brayton cycle using evolutionary algorithm and decision making. Ain Shams Eng J 7:741–753